CHAPTER 5

DESIGN AND ANALYSIS OF A COLLECTOR FOR THE 42 GHz 200kW GYROTRON*

*Part of this work has been published as:

S. K. Sharma, Sudha Gupta, U. Singh, N. Sahu, N. Shekhawat, D. Srivastava, H. Khatun, M. K. Alaria, P. K. Jain and A. K. Sinha, "Design and development of test collector used in gun-collector module for MIG testing of 42 GHz, 200 kW Gyrotron", Int. J. of Engineering Science and Innovative Technology (IJESIT), Vol. 3. Issue 5, pp. 355-362, September 2014.

5.1 Introduction

Collector is an assembly used in the final stage of the device for the collection of unspent electrons in the gyrotron or any other electron beam device. The electron beam generated from the magnetron injection gun (MIG) transfers a fraction of its energy to the RF field in the interaction structure and the remaining electrons proceed further down the device. Obviously, an assembly is needed to collect the remaining energy left with the electron beam after beam wave interaction process and this assembly is usually called as the beam collector or simply collector. The electrons collected on the collector is called as the spent electron beam. Although the electrons lose some of its energy to the RF field, however, a sufficient kinetic energy still remains in the spent electron beam depending upon the efficiency of the device. The collector is supposed to handle (dissipate) a large power coming from the spent electron beam as due to conversion of the kinetic energy of the electron beam remaining in the spent beam into the thermal energy which leads to the increase in temperature of the collector assembly. Thus, the collector design should be such that there is not much rise in the temperature of the collector to avoid the melting or even softening of the collector material. Normally, collector is supposed to be cooled, particularly, in a high power gyrotron to provide the smooth flow of heat flux from the inside surface to the outside surface of the collector. Thus, normally, the oxygen free high conductivity (OFHC) copper is used as the collector material due to its high thermal conductivity capability along with other features, like, vacuum compatibility, ease of availability, etc. The schematic view of gyrotron showing electron beam collector and other components is presented in Fig. 1.1.

In a gyrotron, the electron beam profile is designed to strike on a large extended length or surface around middle portion of a collector so that there is no back reflection towards the interaction structure from the collector as well as there is no bombardment of electrons on the gyrotron window, particularly in an axial type of gyrotron. Design of electron beam spread is made is in such way that the wall loading for collector surface should not be more 2 kW/cm^2 [Edgecombe (1993), Ling *et al*. (2000), Thumm (2010), Thumm (2011)].

Collectors are normally of two types (i) undepressed collector and (ii) depressed collector, respectively [Gilmour (1986), Kartikeyan *et al*. (2004)]. In the undepressed collector, the collector and the device body (control anode) are at the same potential while at different potentials in the depressed collector. The depressed collectors help to increase the overall efficiency of the gyrotron tube in comparison to the undepressed collector [Gilmour

(1986), Kartikeyan *et al.* (2004)]. Single stage depressed collectors have been successfully used in gyrotron increasing the overall device efficiency to above 50% [Edgecomb (1993), Thumm (2010), Thumm (2011), Ling *et al*. (2000)]. It is of interest to mention that inspite of the benefits of efficiency enhancement through depressed collector systems, its use is limited, particularly in a gyrotron due to (i) technological complexity in its fabrication resulting from the use of different electrodes and ceramics in between, (ii) complex power supply for operation of applying different potentials on various electrodes of collector, (iii) cost factor, etc. Thus, for the technological simplicity, the undepressed collector is selected for use in the 42GHz, 200kW gyrotron under development.

Electron beam experiences a reduced magnetic field after the beam-wave interaction and thus its Larmor radius gets increased in the collector region and thereby having a natural tendency to strike on the collector surface. However, it is also required to have a magnetic system around the collector too for the proper electron beam spread for the reduced power dissipation on the collector surface. Further, as mentioned earlier, due to landing of the high energetic spent electron beam on the collector, a large heating of collector surface becomes an issue and a good cooling mechanism around the collector is certainly required. Cooling is done normally by the conventional cooling method where water is circulated around the collector to transfer the heat through it. Thus, the collector system may be supposed to consist of electron beam, collector, coolant, cooling duct and magnet solenoid coils (Fig. 5.1). It is also clear that the proper electron beam spread is achieved with the optimization of collector and surrounding magnet parameters through an electron beam dynamics tool. Similarly, the collector thermal behavior is achieved through the optimization of collector thickness and cooling system parameters with the help of a thermal analysis tool. Therefore, the collector system needs two design aspects related to electrical design and thermal design, respectively (Fig. 5.2).

Design of any component needs a design flow and thus developed for a collector and discussed in Section 5.2. The design flow is applied to a typical collector for 42GHz, 200kW gyrotron under development. Section 5.3 presents the electrical design while Section 5.4 elaborates the thermal design.

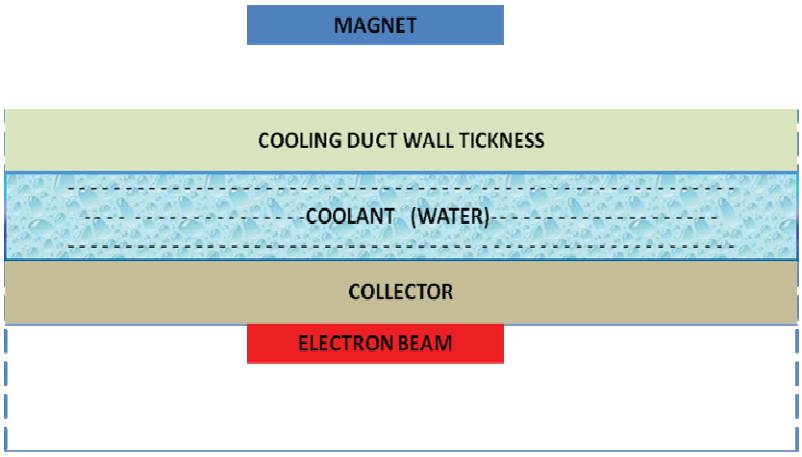

Fig. 5.1: Schematic view of the gyrotron electron beam collector system.

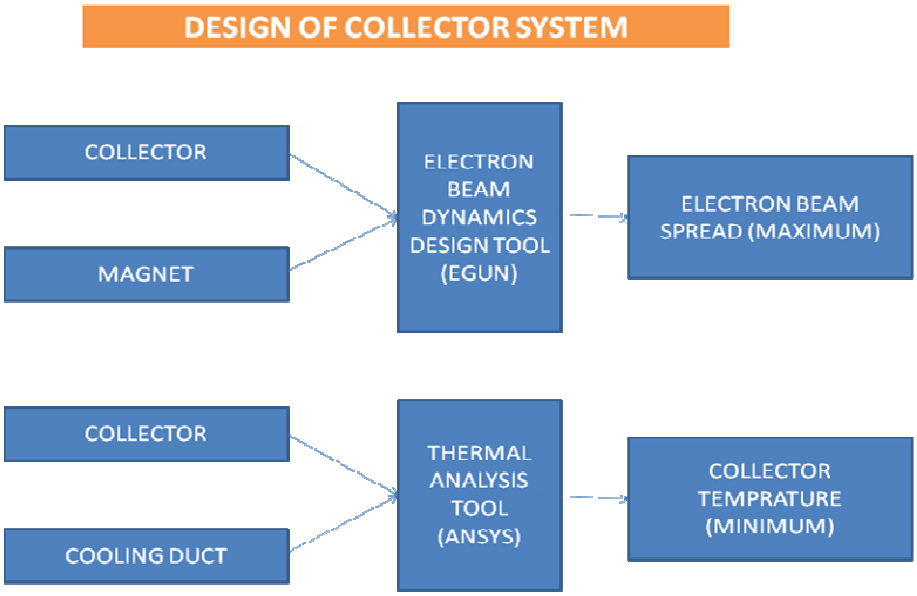

Fig. 5.2: The approach followed for design of the collector system of the gyrotron.

5.2 Collector Design Methodology

Design flow for the gyrotron collector is developed and pictorially presented in Fig. 5.3. The design methodology is based upon the electrical and the thermal design models shown in Fig. 5.2. It covers both the electrical design for prediction of electron beam spread and the thermal design for estimation of temperature profile of the gyrotron collector. The design flow starts from the basic input data, that is, the total spent beam electron beam power required to be dissipated (sub-section 5.2.1). Then, from these collector data, the electron

beam spread is achieved through the optimization of collector dimensions particularly radius and length and magnetic system particularly magnetic strength and location by using the commercial numerical code EGUN (Section 5.3) [Hermannsfeldt (1979)]. Finally, the optimized electrical design of collector is subjected to the thermal analysis with the help of the commercially available numerical code 'ANSYS' (Section 5.4) [ANSYS (2010)].

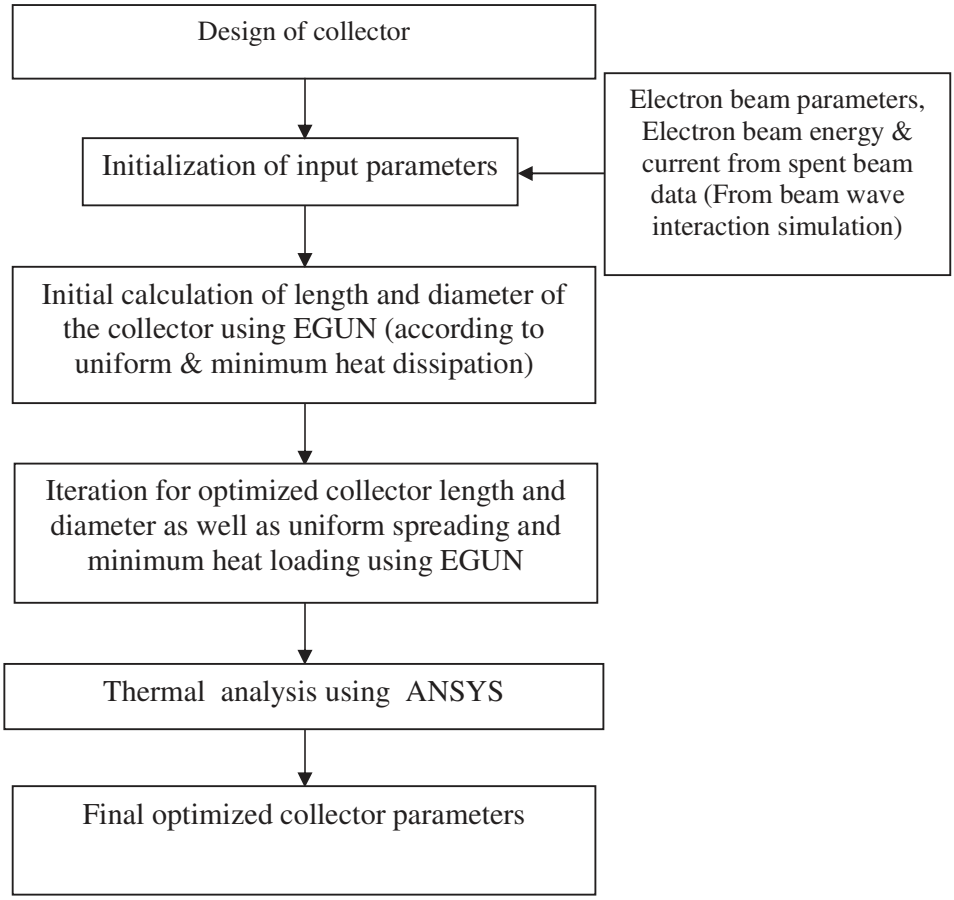

Fig. 5.3: Initial design flow steps for the electron beam collector of the gyrotron.

5.2.1 Initial design

The electron beam spread is the landing area of the spent electron beam. The design of the collector is carried out to get the maximum beam spread so that the power dissipation density remains the minimum leading to the minimum temperature on the collector surface. The electron beam spread can be initially achieved through the estimation of collector dimensions by using the following expression:

$$P_{den} \times A_{sur} = P_{tot} \tag{5.1}$$

and $$A_{sur} = 2\pi R_{col} L_{col} \quad , \qquad (5.2)$$

where P_{den} is the power density on the collector, A_{sur} is the surface area of collector, R_{col} is radius of collector, L_{col} is length of collector and P_{tot} is total power dissipated, respectively. By considering the power density of 250W/cm^2 and total power dissipated on collector surface of 450kW, the initial values of radius and length of collector are calculated through (5.1) and (5.2). A number of combinations of initial designs of collector are obtained and presented in Table 5.1. From these data a set of values of collector radii and lengths are selected for the design of the collector of the gyrotron.

Table 5.1: Initial estimation of radius and length of the collector.

S.N.	**Radius (R_{col}) (mm)**	**Length (L_{col}) (mm) with P_{den} = 250 W/cm^2**
1.	25	1146.5
2.	30	955.5
3.	35	820.4
4.	40	716.6
5.	45	636.9
6	50	573.3
7	55	521.1
8	60	477.7

5.3 Electron Beam Spread Analysis

Electron beam analysis is required for the electrical design of collector, which helps in getting the maximum electron beam spread on the gyrotron collector inner wall surface. This is carried out with the help of a commercially available and widely used the electron beam analysis code EGUN [Hermannsfeldt (1979)]. Before the analysis, some design goals are set-up for the optimized collector design. These goals defined as the collector length should be such that electron beam should not touch the collector end, the electron beam spread should be maximum and should be around the centre of the gyrotron collector, the magnetic field value around the collector should be as low as possible, the coolant temperature should not be more than 50°C (during thermal analysis), etc. The design of the undepressed collector for the 42GHz gyrotron is carried out in steps from the output end of the cavity to the

collector domain using a trajectory code EGUN [Hermannsfeldt (1979)]. The analysis of electron beam collector helps to optimize the collector dimensions and to achieve the maximum electron velocity spread on collector surface through the magnetic field optimization.

It is of interest to mention that the non-adiabatic decompression method is used to design an undepressed collector for the 42GHz, 200kW gyrotron. In this method, the longitudinal momentum of the electron is converted into a transverse motion resulting in an increase of the Larmor radius. This is achieved with the help of an additional solenoid coil in the collector region of the gyrotron. The above-mentioned method helps to reduce the collector dimensions such that the peak wall loading remains within the technical handling limits.

The electron beam simulation is carried out using 30 beamlets with the real energy distribution of the beam. The beamlets represent the beam power equivalent to the 450kW. The electron beam energy is initially generating 650kW from electron beam source and after the beam wave interaction 200kW RF power is grown and taken out of the gyrotron window. Therefore, the rest 450kW power is remained with the electron beam and needs to be dissipated on the inner surface of the collector. As mentioned, the analysis and design of the undepressed collector for the 42GHz gyrotron needs to run in steps from the output end of the cavity to the collector domain. This is necessary to generate realistic beamlet information from the energy dispersion data used in the code. Fig. 5.4 shows the spent beam profile at collector surface without the use of any additional magnetic coil around the collector. Fig. 5.4 clearly presents the overall gyrotron device, for the sake of completeness, starting from electron beam source, that is, magnetron injection gun (MIG), microwave absorbing cavity, that is, beam tunnel, interaction structure, that is, cavity, nonlinear taper and collector along with the main magnetic field profile having the maximum value at the gyrotron cavity. The dimensions of the MIG and cavity are already discussed in Chapters 2 and 4, respectively. The dimensions of the beam tunnel and nonlinear are also optimized [Singh *et al*. (2011), Kumar *et al*. (2011)] . The dimensions of collector is optimized as length equal to 800mm and radius of 42.5mm after lot of iterations to get the best possible landing of the spent electron beam without magnetic field.

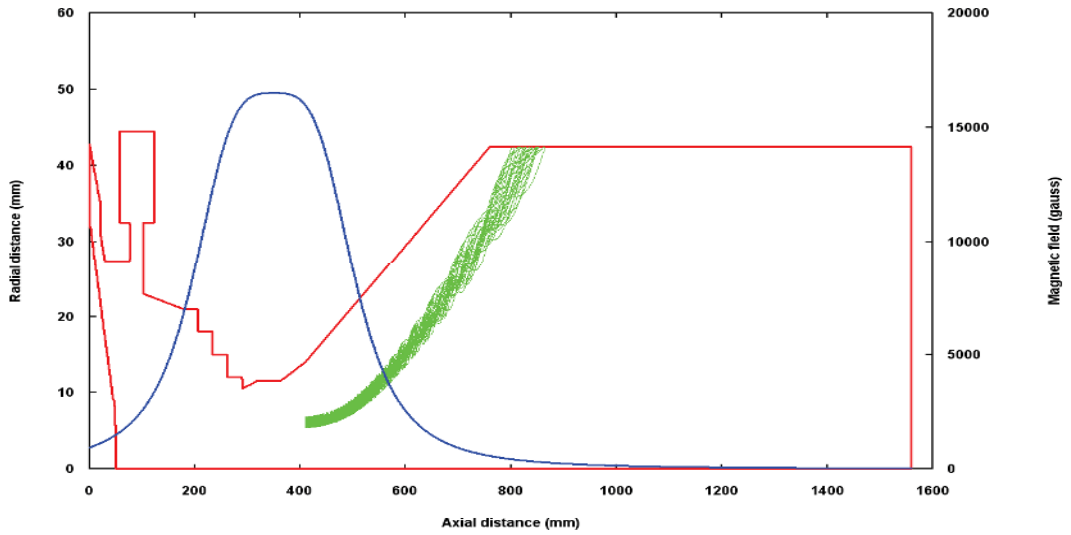

Fig. 5.4: Spent beam profile at the gyrotron collector surface without the collector magnet.

It is found that the magnetic field plays an important role in the optimization of the length and radius of the collector. The magnitude and position of the magnetic field affects the beam spread on the collector surface. Thus, the electron beam analysis is carried out with the help of EGUN code to study the beam spreading over the collector surface under influence of the magnetic field. To achieve technical constraints of the power dissipation capability and other constraints related to dumping of electron beam on the collector surface, the collector dimensions and magnetic field distribution in the collector region are changed accordingly. The steps taken in the design optimization of undepressed collector are as follows: (1) initially collector length is estimated according to maximum heat dissipation, (2) then, a study of tapered length and tapered input radius is carried out to optimize the collector length and collector radius, at constant magnetic field on which maximum spread is achieved, (3) in the next step electron beam energy and magnetic field are varied to achieve the maximum spread on the collector and to optimize the radius of collector and (4) then finally the numbers and position of the coils as well as ampere-turns of each coil are optimized to achieve maximum spread over collector surface. In this manner, the optimizations of length and radius of the collector along with position and axial magnetic field strength of solenoid magnetic system around collector to achieve maximum beam spreading are carried out.

It is found that a two layer system of magnet systems yields the optimized result of the electron beam spread of 330mm at around centre of collector. Figs. 5.5 - 5.6 present some typical values of electron beam spreads in the studies of collector design. For the uniform beam spread equal to 330mm achieved in Fig. 5.6 is selected for further study related

to the thermal analysis study. Table 5.2 shows the values of the radial and axial positions of the magnetic systems along with the magnetic fields. It is also found that the optimized electron beam spread is achieved with the equal values of magnetic field values of both magnetic system located at the same axial positions but the different radial positions. The three magnetic field systems are optimized to be axially located at 935mm, 1045mm and 1175mm, respectively, which present the distances from the collector opening end as 185mm, 295mm and 325mm, respectively as the collector end is at 750mm from the beam spread one end location. The values of amp-turn of Table 5.2 gives the product of current in ampere and number of turns as per requirement in analysis through EGUN code.

Table 5.2: Position and magnetic field values of the magnet coils around collector.

	Axial position (mm)	**Radial Position (mm)**		**Magnetic field value of each magnet (Gauss)**	**Ampere turns (Amp-turn)**
		Layer 1	**Layer 2**		
Magnet 1	935	130	140	369	1270
Magnet 2	1045	130	140	323	1550
Magnet 3	1175	130	140	245	1270

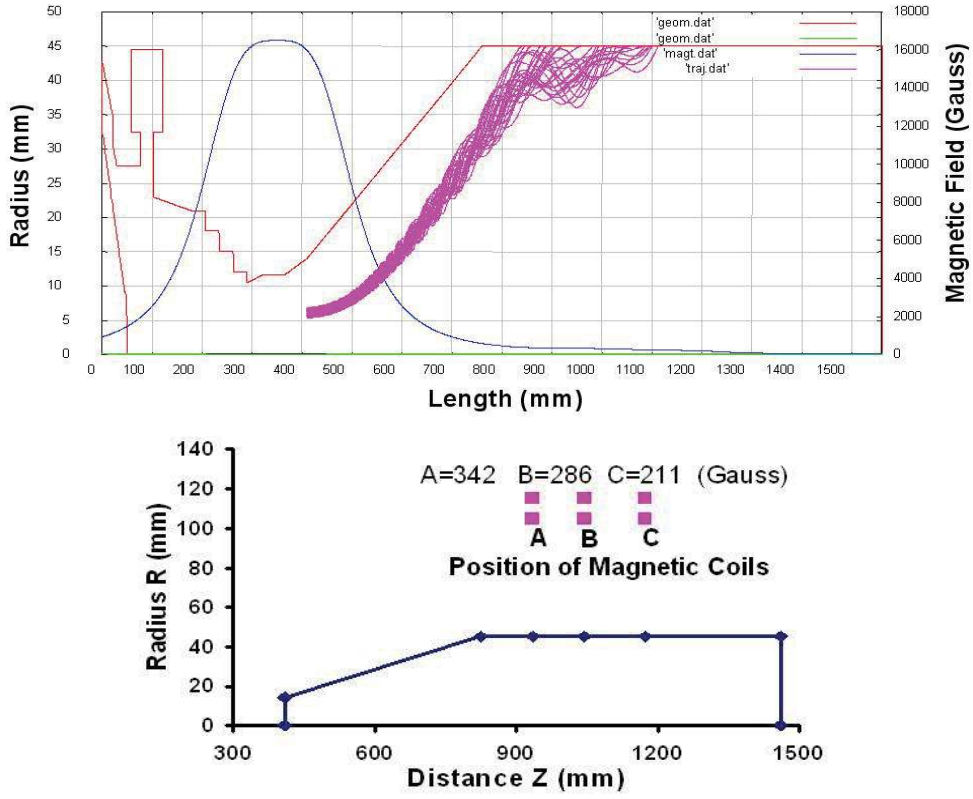

Fig. 5.5: Magnetic coils position and beam spread on the surface of collector (collector length = 800mm, collector radius = 45mm, non-linear tapered length= 350mm, electron beam spread = 272mm, wall loss = 0.617kW/cm^2).

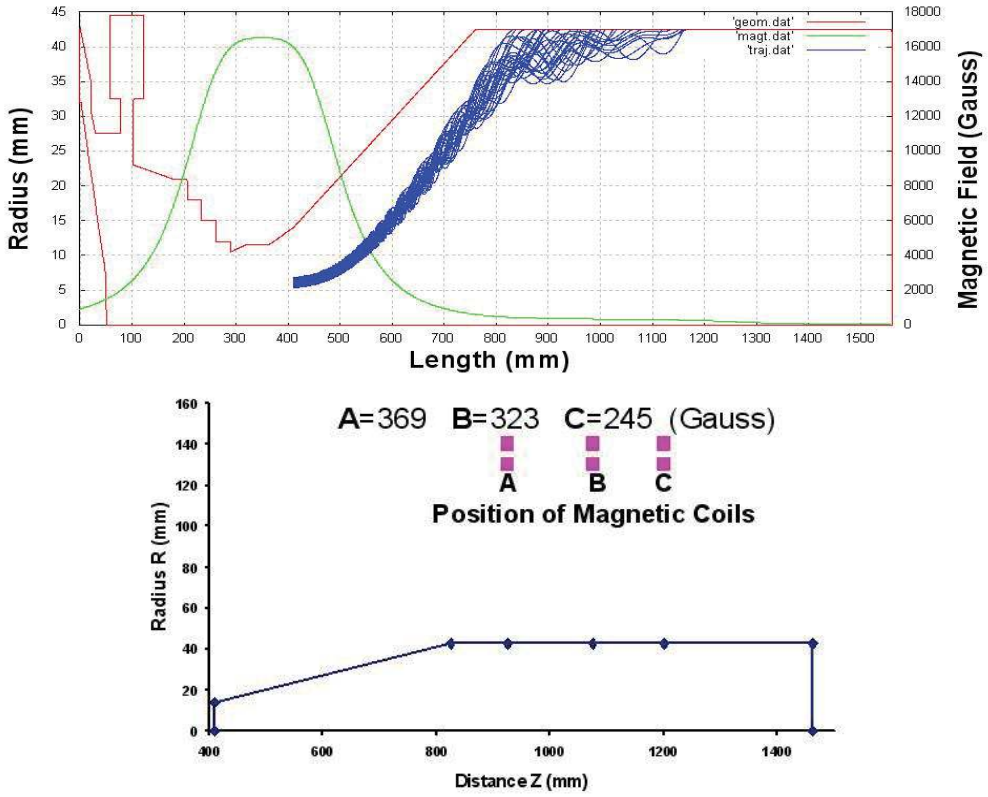

Fig. 5.6: Magnetic coils position and beam spread on the surface of collector (collector length = 800mm, collector radius = 42.5mm, non-linear tapered length = 350mm, electron beam spread = 330mm, wall loss = 0.510kW/cm^2).

5.4 Collector Thermal Analysis

A system is heated under the influence of some sort of the heat flux. This is also true for the gyrotron collector. As mentioned earlier, the high energetic spent electron beams are incident on the collector surface and thus the temperature of the collector gets increased. It is always preferable to maintain the temperature of the collector within the limit, so that there is no thermal stress on the collector body during the device operation. The thermal behavior is estimated through thermal analysis. Two types of thermal analyses can be performed: (i) steady state analysis and (ii) transient analysis. The equilibrium temperature distribution within a structure is estimated through a steady state thermal analysis to determine steady heat flow rates. A transient thermal analysis is performed to determine the temperature distribution in a structure as a function of time to predict the rate of heat transfer or heat storage in the system. The heat load can be applied on the wall surface in the form of heat flux or heat generation rate or specified temperature in each of the thermal analyses. For the thermal analysis through ANSYS code, at first, the analysis flow is discussed (sub-section

5.4.1). Then, the thermal analysis of collector for the 42GHz, 200kW gyrotron is carried out to estimate the safe collector temperature (sub-section 5.4.2).

5.4.1 Thermal analysis flow

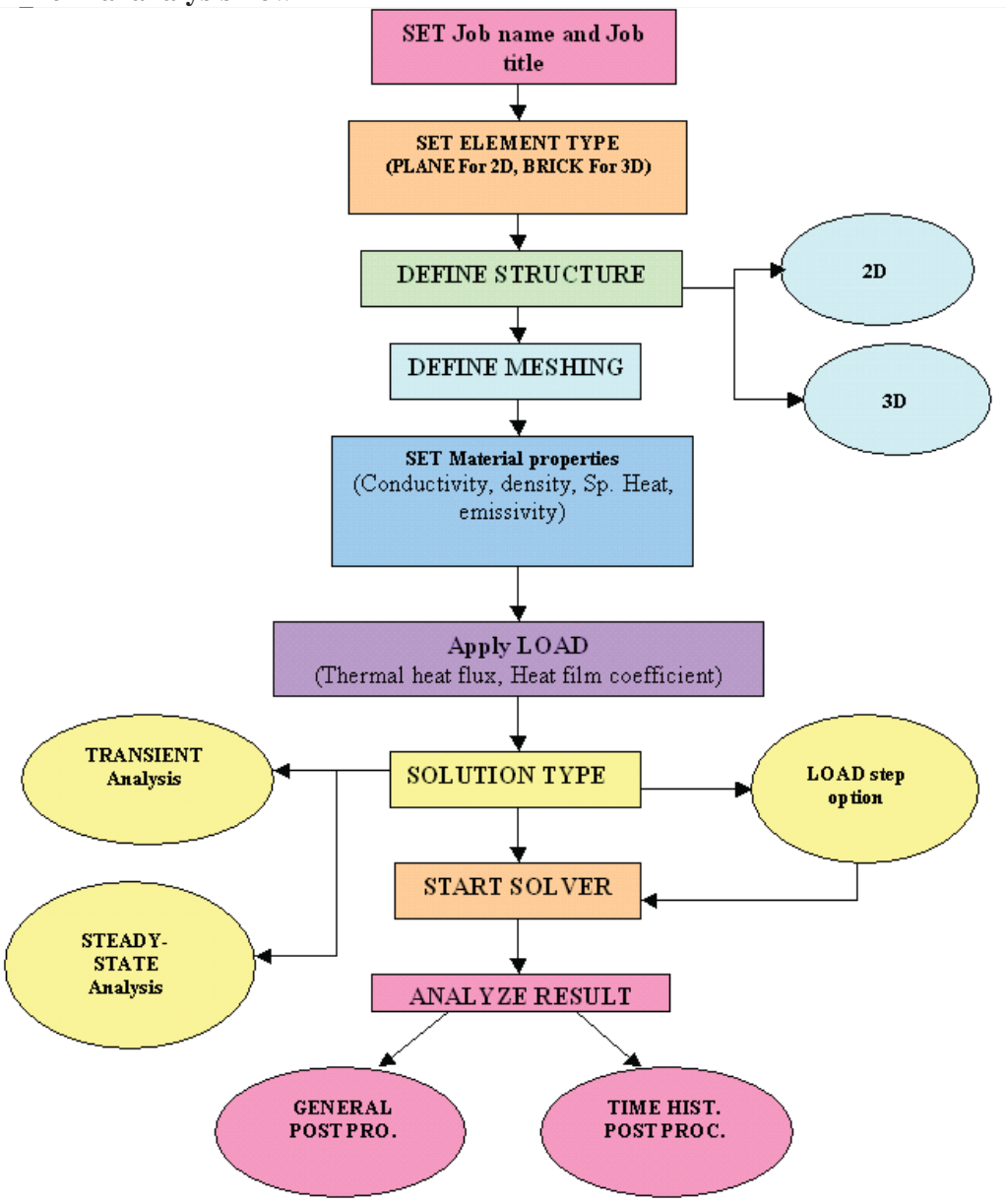

Fig. 5.7: Flow diagram for the thermal analysis using ANSYS code.

The finite element based commercial code "ANSYS" is used to carry out the thermal analysis of the collector for the 42GHz, 200kW Gyrotron [ANSYS (2010)]. Fig. 5.7 shows the flow diagram for this thermal analysis using ANSYS code. The flow diagram clearly shows that the input parameters, such as, conductivity, specific heat, emissivity, etc. of the collector material, are required for the analysis. The electron beam spread obtained through electrical design (Section 5.3) is employed to estimate the heat load on the collector surface.

Since, 200kW electron beam is employed in RF power generation in the interaction structure out of 650kW of the electron beam generated from the MIG electron beam source and thus 450kW is the electron beam power remains in the spent electron beam and required to be dissipated through the collector surface of the gyrotron.

Various input parameters used in the thermal analysis have its distinct role in the thermal analysis. For example, specific heat is used as the input parameter to account for the heat storage effects. The heat is generated when the high energy beam strikes at the collector surface. This generated heat increases the temperature of the collector material and may deform the collector structure. The collector starts melting, if the collector temperature becomes equal to the melting point of the collector material. Thus, it is necessary to effectively remove out the heat generated from the collector, so that the smooth operation of the gyrotron can take place. For the collector materials, the important aspects can be defined, such as, the materials should be non-magnetic to avoid any change in the electron beam dynamics, high melting point to avoid melting or softening due to handling of high energetic electron beam, having high mechanical strength for robustness, having vacuum capability for handling electron beam transfer in vacuum, etc. OFHC copper is normally used as the collector material due to its low loss properties.

5.4.2 Estimation of the collector temperature

Using the flow diagram shown in Fig. 5.7, thermal analysis of the collector for the 42GHz, 200kW gyrotron under development process is carried out with the help of ANSYS software [ANSYS (2010)]. For this purpose, at first, on the basis of electrical design (sub-section 5.2), the collector geometry is synthesized in ANSYS (Fig. 5.8) Then, the thickness of the collector wall, the collector shape and the water flow rate are optimized. The dimensions of the collector, used in the ANSYS simulations, are kept the same as 85 mm diameter and 800mm length, as finalized in Section 5.3 (Fig. 5.8).

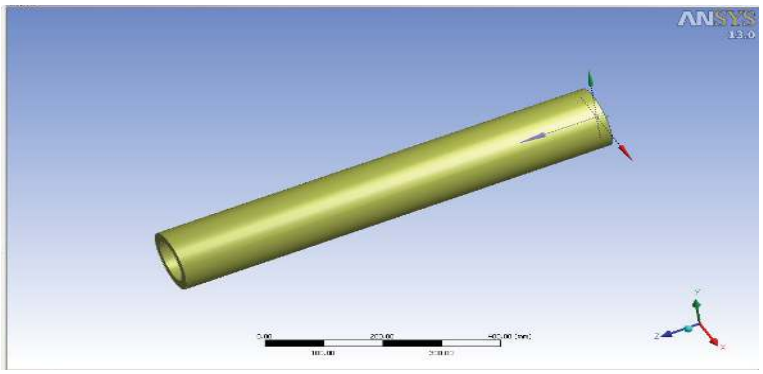

Fig. 5.8: 3D view of collector structure in ANSYS simulation.

The oxygen free high conductivity (OFHC) copper, as mentioned earlier, is normally used as the collector material and for the cooling system water is used as the coolant for the thermal study of collector of the 42GHz, 200kW gyrotron. The thermal and mechanical properties of OFHC copper and water are given in Tables 4.3 and 4.4, respectively. After meshing of the collector geometry, the material properties are applied. After that, the loads and the boundary conditions are applied. As discussed in Section 5.2, the optimized magnetic field strengths of the three magnet coils to achieve 330mm spread are 369G, 323G and 245G, respectively. The computed average wall loss is 0.510kW/cm^2 which is within the technical limits. The peak power density of 330mm spread is 1.08kW/cm^2. However, in the thermal analysis, for the sake of convenience, the average wall loss is applied on the collector surface along the length or surface equivalent to the electron beam spread.

Table 5.3: Thermal and mechanical properties of OFHC copper.

Parameter	**Unit**	**Value**
Density	kg/m^3	8960
Thermal conductivity	W/m.K	334
Emissivity	--	0.4
Specific Heat	J/ kg.K	385
Young's Modulus	GPa	110
Poisson's Ratio	--	0.33
Thermal expansion coefficient	/K	17E^{-6}

Table 5.4: Properties of water as a coolant for the cooling system.

Parameter	**Unit**	**Value**
Density	kg/m^3	998.21
Viscosity	N S/m^3	0.855×10^{-3}
Conductivity	W/m.K	0.58

For the design of cooling duct a simple cooling duct/ cylinder made of stainless steel 304 is used around the collector through which water is flown. The cooling is carried out by conventional cooling method in which the heat transfer from the inner wall to the outer wall of the undepressed collector takes place through conduction mechanism and from outer wall to the coolant by the convection mechanism.

After assigning the material properties, limiting values of the coolant temperature and the inner collector surface temperature are assigned. For this situation, at first, the heat film

coefficient is optimized for various coolant flow rates to achieve the best (minimum possible) value of collector inner and outer surface temperatures, where the heat film coefficient depends upon the coolant material properties, the coolant flow type and flow rate, the cooling duct dimension, etc. The heat film coefficient (h) can be expressed as [Incropera *et al.* (1990)]:

$$h = k\, Nu / D_h \quad , \tag{5.3}$$

where, k is the thermal conductivity of coolant, D_h is hydraulic diameter of cooling duct. The hydraulic diameter is also used to calculate the pressure loss in a duct / pipe. The hydraulic diameter is not the same as the geometrical diameter in a non-circular duct / pipe and can be calculated through the relation given as:

$$D_h = 4\, A / p \quad , \tag{5.4}$$

where A is the area section of the duct and p is the wetted perimeter of the duct. The hydraulic diameter is the diameter of the flow cross-sectional area and the hydraulic diameter of a circular duct or tube with an inside cylinder or tube can be expressed from (5.4) as:

$$\begin{aligned} D_h &= 4\, (\pi\, r_o^2 - \pi\, r_i^2) / (2\, \pi\, r_o + 2\, \pi\, r_i) \\ &= 2\, (r_o - r_i) \end{aligned} \tag{5.5}$$

where r_o and r_i are respectively the outer and inner radii of cooling duct. Nusselt number (Nu) occurring in (5.3) may be expressed as:

$$Nu = 0.023 (Re)^{0.8} (Pr)^{0.4} \tag{5.6}$$

where R_e is Reynolds number which depends upon coolant type and nature of flow. The Reynolds Number for a duct or pipe can be expressed as:

$$Re = \rho\, u\, D_h / \mu' \tag{5.7}$$

where ρ is the density, u is coolant (water) velocity defining flow rate and μ' is the dynamic viscosity, respectively. The Reynolds number can be used to determine the nature of flow, that is, if flow is laminar, transient or turbulent. The flow is laminar when $Re < 2300$, transient when $2300 < Re < 4000$ and turbulent when $Re > 4000$ [Incropera *et al.* (1990)]:

Further, the Prandtl number (P_r) is a dimensionless number approximating the ratio of momentum diffusivity (kinematic viscosity) and thermal diffusivity. It may be simply defined as:

$$P_r = c_p\, \mu / k \quad . \tag{5.8}$$

The basic property of water, that is, density, viscosity, thermal conductivity, etc. change with the rise in temperature and therefore, in the thermal analysis, the changed values of these parameters are used. Figs. 5.9 - 5.10 present the effect of temperature on some properties of water [Incropera *et al*. (1990)].

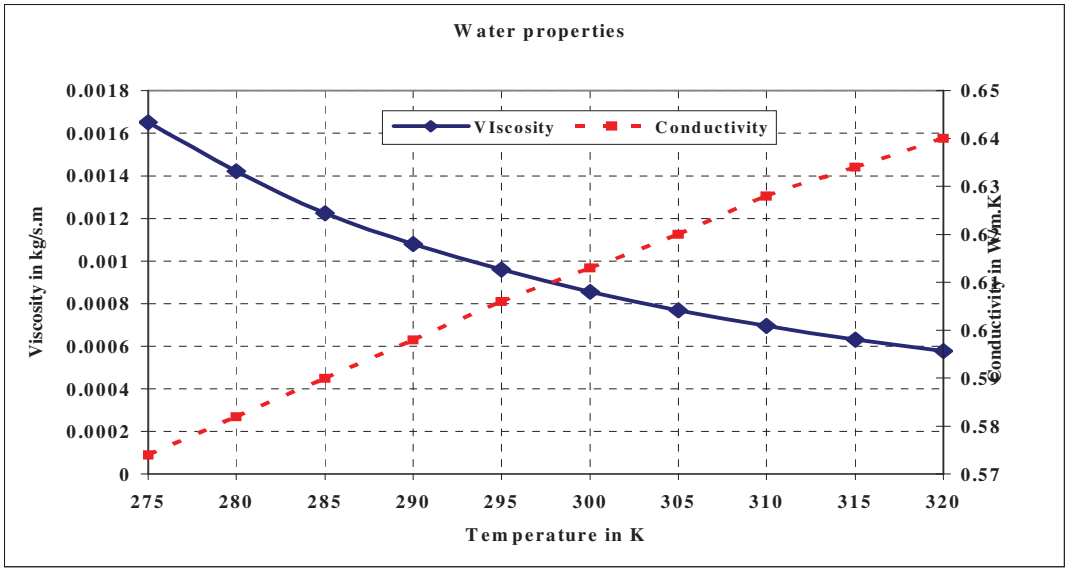

Fig. 5.9: Variation of water viscosity and conductivity at different temperatures.

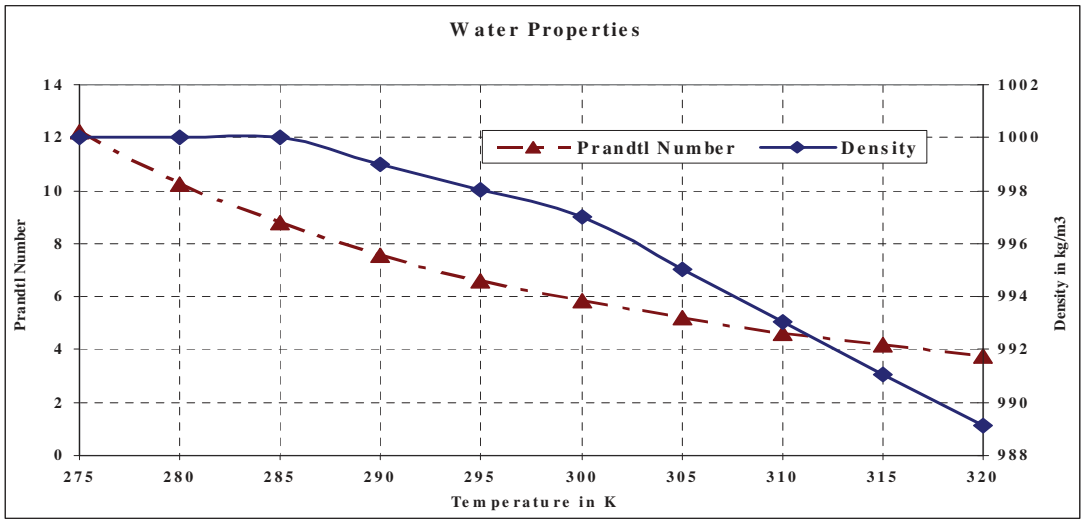

Fig. 5.10: Variation of Prandtl number and density at different temperatures.

After finding the optimized heat film coefficient, the hydraulic diameter is estimated for a given coolant flow rate through (5.3) and (5.4). In this respect, a typical plot is obtained between water flow rate and hydraulic diameter for various values of heat film coefficients (Fig. 5.11). It is clear from Fig. 5.11 that the hydraulic diameter increases with increase in

the water flow rate at a given value of heat film coefficient whereas hydraulic diameter decreases with increase of heat film coefficient at a given water flow rate. The estimation of the proper heat film coefficient also helps in the design of grooves, if needed, on the collector surface. From the simulated results, it is also found that the thermal management is better in case of the axial grooves compared to the plane outer surface collector (Fig. 5.12). However, in both situations, the collector surface temperatures decrease with the increase of the heat film-coefficient.

The thermal analysis of collector is carried out with the axial grooves. The axial grooves are also used on the outer surface of the collector for getting lower surface temperature (Fig. 5.12). It is clear from Fig. 5.12 that with the use of axial grooves, the temperature of the collector surface is sufficiently reduced. Furthermore, the study is made for optimizations of various values of the coolant parameters and the axial grooves with collector radius = 42.5mm, collector length = 800mm, spread length = 330mm, collector thickness = 20mm.

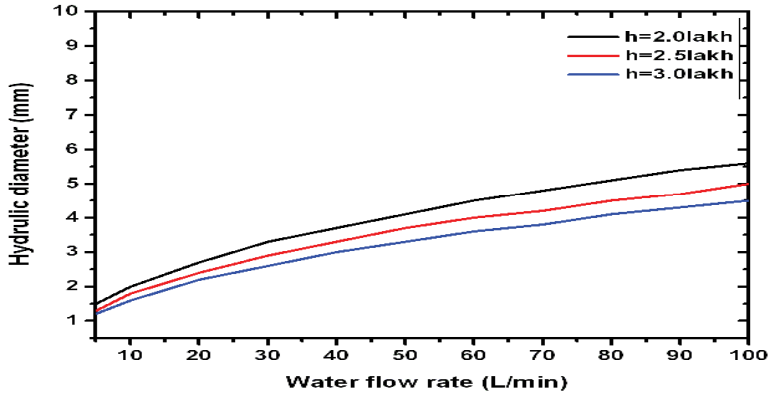

Fig. 5.11: Variation of hydraulic diameter with respect to water flow rate for different values of heat film coefficient (h).

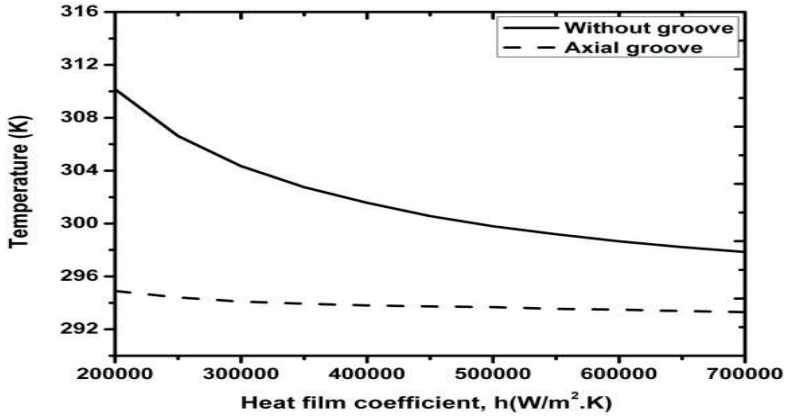

Fig. 5.12: Variation of collector outer surface temperature with respect to heat film coefficient with and without groove on the collector outer surface.

The typical and optimized values of axial grooves are found by keeping temperatures of outlet water coolant within the limit of around 10^0C. The optimized values are given as number of axial grooves on outer surface = 18, groove thickness = 4mm, groove height = 16mm, groove width = 4mm and space between two grooves = 16.5º. Two cases of power dissipations are studied, such as, (i) 450kW dissipated spent electron beam power when 200 kW RF power is generated and (ii) total 650kW spent electron beam power when no RF power is generated. The studies are further carried for various inlet water temperatures, such as, 288°K - 293°K and hydraulic diameters ranging from 4.0 - 4.5 - 5.0mm diameter. It is found that in both cases, the temperatures of both inner and outer surfaces continuously decrease with increase in water flow rate in all the situations. It is always desired to achieve the inner collector surface temperature around or less than 473°K which is easily obtained through these simulated results. Figs. 5.13 and 5.14 presents the typical thermal analysis results for both situations related to 450kW and 650kW power dissipations.

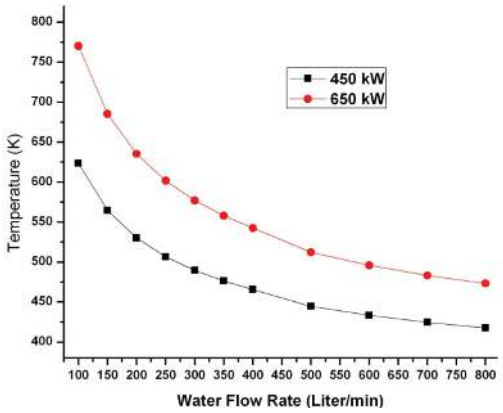

Fig. 5.13: Collector inner surface temperature versus water flow rate (axial grooves = 18, water temperature 293°K, beam spread = 330mm, hydraulic diameter = 4.5mm).

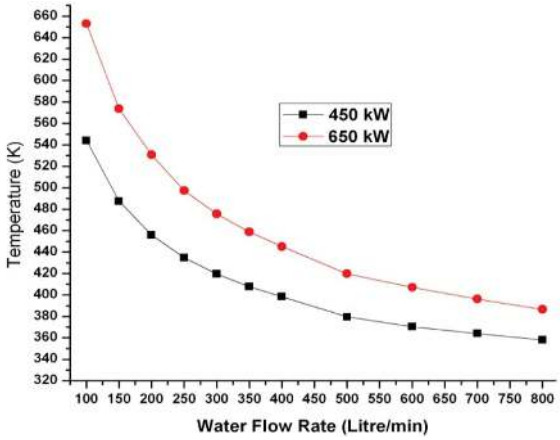

Fig. 5.14: Collector outer surface temperature versus water flow rate (axial grooves = 18, water temperature 293°K, beam spread = 330mm, hydraulic diameter = 4.5mm).

5.4.3 Transient thermal study

The transient thermal study gives the idea about the maximum temperature rise before the steady state. Keeping this into consideration, the transient study is also carried out for various situations. Some typical results are presented in Figs. 5.15 and 5.16 for 450kW and 650kW power dissipations for different water flow rates showing the temperatures of inner and outer surfaces of the collector. These simulated results, makes is clear that in all cases the temperature rise time becomes constant after 2-3 sec.

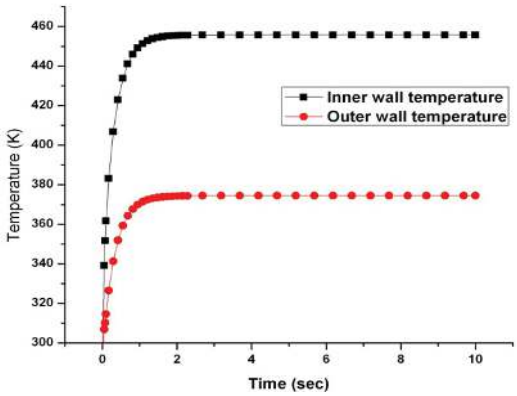

Fig. 5.15: Collector temperature versus time (axial grooves = 18, water temp 293°K, beam spread = 330mm, hydraulic dia = 4.5mm, water flow rate = 800L/m, power dissipation = 450kW).

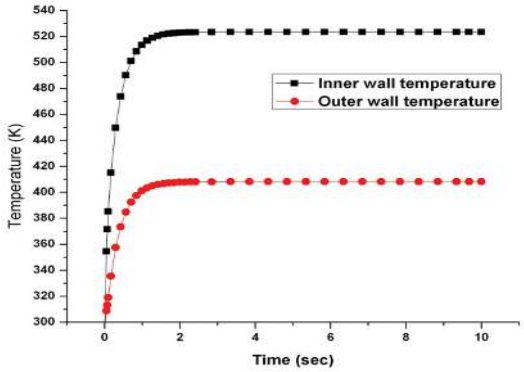

Fig. 5.16: Collector temperature versus time (axial grooves = 18, water temp 293°K, beam spread = 330mm, hydraulic dia = 4.5mm, water flow rate = 800L/m, power dissipation = 650kW).

5.5 Characterization of a Test Collector

The gyrotron gun is tested through fabrication of a gun-collector module which needs a component to collect the electron beam generated from the cathode of the electron gun. The collector designed for gyrotron is not a feasible idea for use in the test of the MIG. The collector used in the gun-collector module is normally called as a test collector which is reduced dimensioned collector and it is sufficient for the purpose of testing of MIG. Since, the test of MIG is planned for the duty cycle only upto the maximum 0.2% duty cycle of the required electron beam power only and thus the test collector size is kept equal to 150 mm

length, 100mm outer mm and 10mm thickness. But, however, the material of test collector is kept the same as OFHC copper as planned for the actual gyrotron collector (Sections 5.2 and 5.3). The suitability of power handling capability of test collector is carried out through the thermal analysis with the help of ANSYS code to see the effects of the heat power loss on the collector inner wall and also the ambient heat film coefficient. Dissipated heat power has been varied from 50W to 2500W in steps of 50W and at each dissipated heat power the ambient heat film coefficient is varied from 100W/m^{2}K to 1000W/m^{2}K in steps of 100 W/m^{2}K as the heat film coefficient directly provides the ambient environment condition. Figs. 5.17- 5.19 present the typical results of the inner and outer wall temperatures with 100W, 1000W and 2500W dissipated heat powers, respectively. The maximum heat power dissipated is kept equal to 2500W as it is planned to test the MIG in the limited test condition with the available infrastructure. It is found that upto 1000W heat dissipation with him coefficient upto 100W/m^{2}K, the maximum temperature on the collector wall temperature is 200^{o}C and the difference between inner and outer collector wall temperatures is not more than 2^{o}C (Fig. 5.17). Similarly, the maximum temperature with the heat film coefficient equal to around 200W/(m^{2}K) for the forced air convection and the dissipated heat power equal to 2500 W, the maximum temperatures on the inner and outer collector wall are estimated around 280^o C which is within the tolerable experimental evaluation condition (Fig. 5.19). The transient thermal analysis is also carried out to see the steady state temperature rise and a typical result is presented in Fig. 5.20. It is also clear from Fig. 5.20 that after around 10 minutes, the steady state condition is reached with temperature rise upto around 120^{o}C with heat film coefficient equal to 100W/(m^2 K) for dissipated heat power.

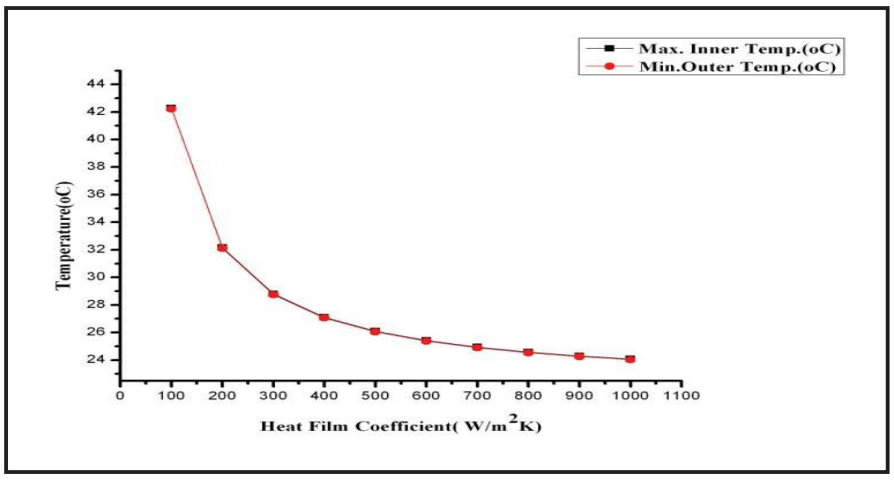

Fig. 5.17: Effect of heat film coefficient on the temp of collector surfaces (Dissipated heat power = 100 W, collector length =150mm, collector thickness = 10mm, collector outer dia = 100mm).

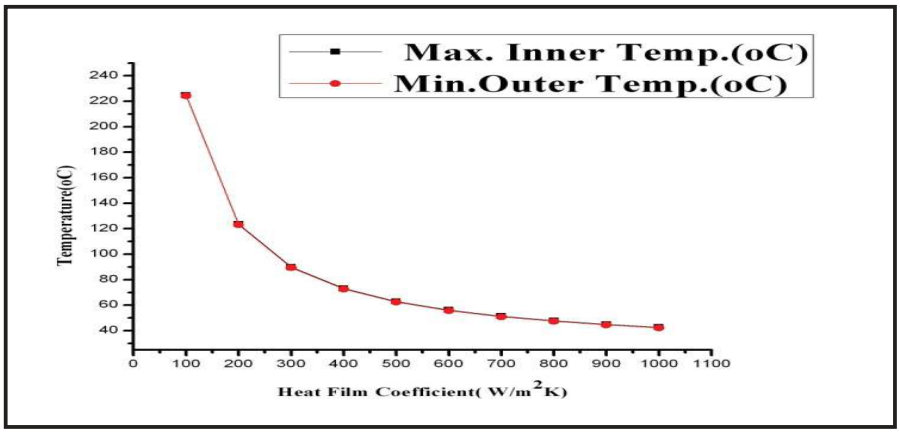

Fig. 5.18: Effect of heat film coefficient on the temp of collector surfaces (Dissipated heat power = 1000 W, collector length = 150mm, collector thickness = 10mm, collector outer dia = 100mm).

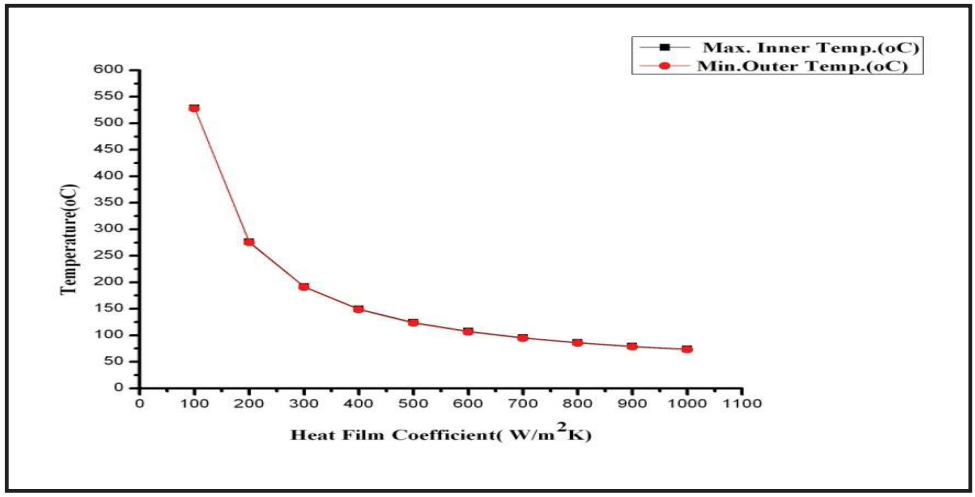

Fig. 5.19: Effect of heat film coefficient on the temp of collector surfaces (Dissipated heat power = 2500 W/m^2, collector length =150m, collector thickness = 10 mm, collector outer dia = 100 m).

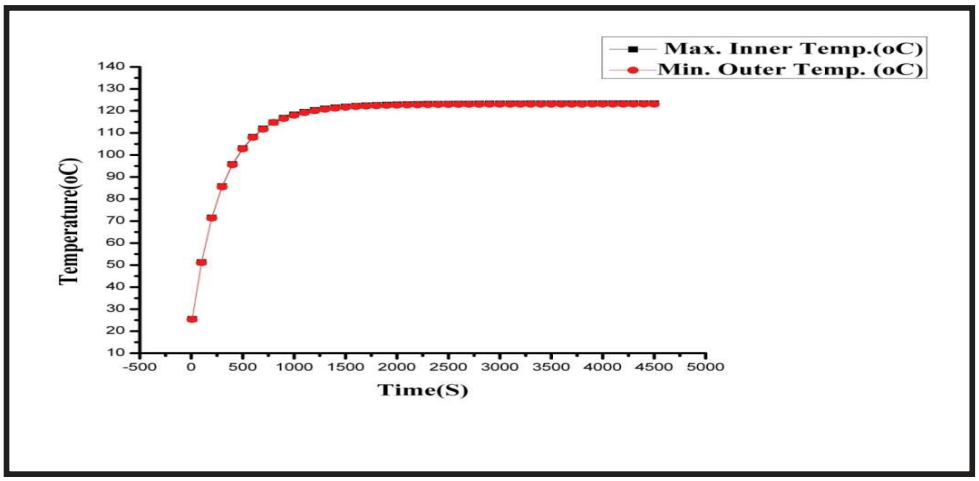

Fig. 5.20: Transient thermal analytical dissipated power =500W, heat film coefficient =100 W/(m^2K) collector length =150mm, collector thickness =10mm, collector outer dia =100mm.

5.6 Conclusion

Collector used for the collection of the spent electron beam in the gyrotron has been studied in this Chapter 5. At first, the initial estimation of collector dimensions, particularly length and diameter have been carried out with the help of analytical expressions subjected to the technical limit of wall loss. Then, a flow chart has been developed and successfully used for the optimizations of the collector dimensions, the collector magnetic field and the electron beam spread for the minimum possible wall loss. The uniform electron beam spread of 330mm was achieved for wall loss of 0.510kW/cm^2 for the collector diameter and length equal to 85mm and 80 mm, respectively. Then, the thermal analysis has also been carried out for the estimations and optimizations of temperatures on the both inner and outer collector surfaces with the reasonable flow of coolant around the collector. Through thermal analysis, it has been established that the employment of grooves on the collector outer surface is found to be the better option from thermal management point of view. As the collector designed for a 42GHz, 200kW gyrotron is not found feasible option for use in the gun-collector module for testing of electron gun due to large size. Thus, a test collector of reduced dimensions of 150mm length and 100mm outer diameter has been designed through both electron trajectory analysis and thermal analysis, respectively.